JOURNAL OF MATERIALS SCIENCE 26 (1991) 2930–2936

Pressureless sintering of AlN–SiC composites

WEN-CHENG J. WEI
The Graduate Institute of Materials Engineering, National Taiwan University, Taipei, Taiwan
RAN-RONG LEE
Ceramics Process Systems Corporation, 155 Fortune Boulevard, Milford, MA 01757, USA

SiC–AlN composites have been successfully pressureless sintered by using commercial SiC and AlN powders with the optimum amount of sintering aid. The important parameters during pressureless sintering, including the amount and type of sintering aids, sintering temperature, sintering period and packing powder have been studied. Yttria was found to be a better sintering aid than alumina or calcia. The yttria sintering aid reacts with AlN and SiC powders and forms a Y–Al–Si–O–N grain-boundary phase to assist densification during pressureless sintering. With 2 wt% yttria, SiC–AlN composites can be pressureless sintered to high density at 2050–2100 °C for 2 h under the firing conditions where alpha-pp packing powder is used during firing. The microstructure and phases of the composites were characterized by using scanning electron microscopy, transmission electron microscopy, energy-dispersive X-ray spectrometry and X-ray diffractometry.

1. Introduction

AlN–SiC ceramics have been studied for the past decade [1–16] because of their potential application at high temperature. Several different methods were used to prepare AlN–SiC composite powders. The first preparation method used was the mechanical mixing of commercially available SiC and AlN powders [3]. The second method was the carbon-thermal reduction of synthetic silica and alumina [1, 2], the third was mixing Si_3N_4 and Al_4C_3 powders [5]. The carbon thermal reduction could yield a smaller particle size and better mixing, but the purity of the alloy powder and the production scale were limited. The $Si_3Al_4N_4C_3$ solid solution had been successfully prepared from Si_3N_4 and Al_4C_3 powders, but the range of the solid solution was limited by their ratio. The mechanical mixing of commercial SiC and AlN powder to prepare AlN–SiC is easy and straightforward. However, different SiC powders affected the formation of the SiC–AlN solid solution [8, 10], and the various particle sizes of SiC and AlN powders were also critical for the formation of the solid solution [8].

After the SiC–AlN ceramic powders were prepared and mixed, hot-pressing was commonly used to consolidate the composite to high density [2–4, 6–15]. Sometimes boron was used as a sintering aid during hot pressing [2], but usually boron was not required [3–4, 6–15]. Typical density of the hot-pressed alloys was 3.08 g ml^{-1}, close to the theoretical density. The hot-pressing method is expensive and can only produce simple geometrical shapes. Although pressureless sintering is better in both aspects, it is not easy to obtain fully dense composites without optimum sintering aids. Not much work has been done on the pressureless sintering of SiC–AlN alloys [1–16]. Huang *et al.* [13] found that with a minor amount of AlN, SiC–Al_2OC could be pressureless sintered to high density because of the liquid phase forming from Al_2O–SiC. A major objective of this current research was to determine appropriate sintering aids for the pressureless sintering of SiC–AlN.

The current study was part of the research for producing *in situ* reinforced composites for high-temperature application. The pressureless sintering of AlN–SiC composites with small amounts of sintering aids, including alumina, yttria and calcia have been studied. Other parameters, such as different types of SiC powder, sintering temperature, sintering time and sintering condition were also investigated. The microstructure and phases of sintered composites were characterized by using X-ray diffractometry (XRD), optical microscopy, scanning electron microscopy (SEM), transmission electron microscopy (TEM) and energy-dispersive X-ray spectrometry (EDS).

2. Experimental procedures

2.1. Raw materials

Three different commercial SiC powders (two beta phase and one alpha phase) and one AlN powder were selected for the study of SiC–AlN alloys. To achieve full density through pressureless sintering, three oxides, yttria, alumina, and calcia, were used as the sintering aid. The physical properties of these powders are listed in Tables I and II.

Although the surface areas of the three SiC powders are similar, about 15 m^2 g^{-1}, the density of the sintered composites prepared from Lonza alpha-SiC is better than that obtained with Starck beta-SiC, as discussed in the following sections.

0022-2461/91 $03.00 + .12 © *1991 Chapman and Hall Ltd.*

TABLE I Chemistry and properties of as-received SiC and AlN powders

	AlN[a]	SiC[b]	SiC[c]	SiC[d]
Al	> 64%	< 0.5%	0.04%	0.018%
N	33.1%	–	–	0.21%
Si	–	bal.	bal.	bal.
C	0.07%	bal.	30.54%	bal.
O	2.0%	< 1.0%	0.85%	0.8%
Free Si	–	< 0.2%	–	0.03%
Free carbon		< 0.5%		0.85%
Fe	0.018%	< 0.1%	0.036%	0.016%
Ca	–	–	0.002%	0.002%
Other metal impurities	< 0.05%	–	–	
Sulphur		–		< 0.5%
Average size (μm)	1.0	0.6 ± 0.2	0.62	0.6
BET ($m^2 g^{-1}$)	5.1–5.2	15 ± 1	15.5	15 +

[a] AlN powder, grade C, Hermann C. Starck, Inc., NY 10017, USA.

[b] Alpha-SiC powder, Carbogran UF-15, Lonza Inc, Engineered Materials, Jersey City, NJ 07304, USA.

[c] Beta-SiC powder, B 10, Hermann C. Starck, Inc., NY 10017, USA.

[d] Beta-SiC powder, HSC 059, Superior Graphite Co., Chicago, Il 60606, USA.

TABLE II Properties of some chemicals used as sintering aids

1. Yttrium oxide finest, H. C. Starck	$C_{tot} = 0.13\%$ FSSS = 0.28 μm BET area = 14.15 $m^2 g^{-1}$ Scott-density = 2.5 $g in^{-3}$
2. A16 alumina, Alcoa	– 325 mesh
3. Calcium oxide, Cerac, Inc.	99.99% pure

2.2. Preparation of the green specimen

A solution composed of iso-propanol, 2.5 wt % Emcol CC-55 (used as a dispersant) and 1 wt % Elvacite 2046 (used as a binder) were pre-mixed for at least 4 h. The powders with the formulations shown in Table III were then dispersed into the solution. The alloys had three different AlN/SiC ratios: 7/3, 5/5 and 3/7. After tumbling the mixture for 16 h, the well-dispersed slurry was slip-cast in a plaster mould with dimensions of 15 mm × 15 mm × 10 mm. The moulded parts were dried at room temperature and then placed in an 80 °C oven to remove the solvent completely.

2.3. Sintering and heat treatment

A high-temperature graphite furnace was used to sinter the SiC–AlN composites. High-purity argon gas with a pressure slightly higher than ambient atmosphere vented the furnace at 0.6 l min^{-1} flow rate. The samples were put into a graphite crucible, and sometimes buried with packing powder.

The sintering profile followed the schedule below:

room temperature to 250 °C, 10 °C min^{-1}
250–400 °C, 3 °C min^{-1}
hold at 400 °C for 1 h
400–1750 °C, 20 °C min^{-1}
1750 °C to sintering temperature, 10 °C min^{-1}
hold at sintering temperature for 1–6 h
cool in furnace, – 40 °C min^{-1}

2.4. Characterization

2.4.1. *Optical microscopy and SEM*

The sintered AlN–SiC ceramics were ground and then polished using various grades of diamond paste. After polishing, the samples were etched with Murakami's reagent and a fused salt mixture of KOH and KNO_3.

TABLE III The formulation (wt%) of AlN–SiC composites and the packing powders (pp)

Sample	SiC (phase)	AlN	Sintering aids
AY2	49% (alpha)	49%	2% yttria
AY4	48% (alpha)	48%	4% yttria
BY2	49% (beta)[a]	49%	2% yttria
BY4	48% (beta)	48%	4% yttria
SBY2	49% (beta)[b]	49%	2% yttria
SBY4	48% (beta)	48%	4% yttria
73Y2	29.4% (alpha)	68.6%	2% yttria
37Y2	68.6% (alpha)	29.4%	2% yttria
AAY2	49% (alpha)	49%	1% yttria + 1% alumina
BAY2	49% (beta)[a]	49%	1% yttria + 1% alumina
AA2	49% (alpha)	49%	2% alumina
BA2	49% (beta)[a]	49%	2% alumina
AC2	49% (alpha)	49%	2% calcia
a-pp	50% (alpha)	50%	–
b-pp	50% (beta)[a]	50%	–

[a] Hermann C. Starck, Inc.

[b] Superior Graphite Co.

The samples were then examined under the optical microscope and SEM.

2.4.2. X-ray diffractometry

XRD analysis was conducted by using commercial equipment at 45 kV and 40 mA. Normally the surface for scanning was cut and ground from the centre of the samples. The scanning rate was 0.5° min^{-1}.

2.4.3. TEM

The specimens were cut into 3 mm discs and polished down to 80 μm thick. Then the thin foils were dimpled to 15 μm and ion-milled by Ar gas. A Jeol 2000FX analytical electron microscope equipped with Kevex "Quantum" energy-dispersive X-ray spectrometers (EDS) was used to characterize microstructure and composition. The EDS system has an ultrathin window and can detect elements boron to uranium.

3. Results and discussion

3.1. Pressureless densification

3.1.1. Sintering aids

Alumina has been reported to be a good sintering aid for pure SiC [17], and yttria and calcia were found to be good sintering aids for AlN [18]. Thus these three sintering aids were chosen for study of the pressureless sintering of AlN–SiC composites. Fig. 1 compares the density of ceramic composites with different sintering aids after they were sintered at 1960–2200 °C. No packing powder was used during these firings. Fig. 1a shows densities of composites with 2 wt % yttria sintering aid; Fig. 1b shows densities of composites with 1 wt % yttria and 1 wt % alumina, and Fig. 1c shows those of composites with 2 wt % alumina. In these figures, the composites using pure yttria as a sintering aid (AY2 or BY2) had higher density than alumina-doped or alumina–yttria-doped samples (AAY2, BAY2, AA2 and BA2). Therefore, yttria was found to be a better sintering aid than alumina.

3.1.2. Polytype of SiC powder

Other important information which can be discerned from Fig. 1 is that composites prepared from alpha-SiC powder (AY2, AAY2 and AA2) have higher density than those prepared from beta-SiC powder (BY2, BAY2 and BA2). The difference in density of these two groups of samples might be related to the stability of SiC polytype at high temperature. It has been reported that alpha-SiC is a more stable phase than beta-SiC, and beta-SiC will transform to elongated alpha-SiC grains at high temperature [19–21]. The transformed elongated alpha-SiC might affect the densification of AlN–SiC composites and cause lower sintered density of AlN–SiC composites. However, further research is required to confirm this idea.

3.1.3. Sintering temperature

The density curves in Fig. 1 also show that optimum sintering temperature was about 2050–2100 °C. Higher sintering temperature did not yield higher density; on the contrary, it lowered the sintered density. The lower density at temperatures higher than 2100 °C might be related to the decomposition of composites at high temperatures; this will be discussed later. The maximum density in these samples under sintering conditions without using packing is only 2.83 g cm^{-3}, which is about 88% TD, and not high enough for real application. Two different methods were tried to improve the sintered density of SiC–AlN composites. The first method increased the amount of sintering aid from 2–4 wt % for better densification. The second method used packing powder to avoid the degradation layer.

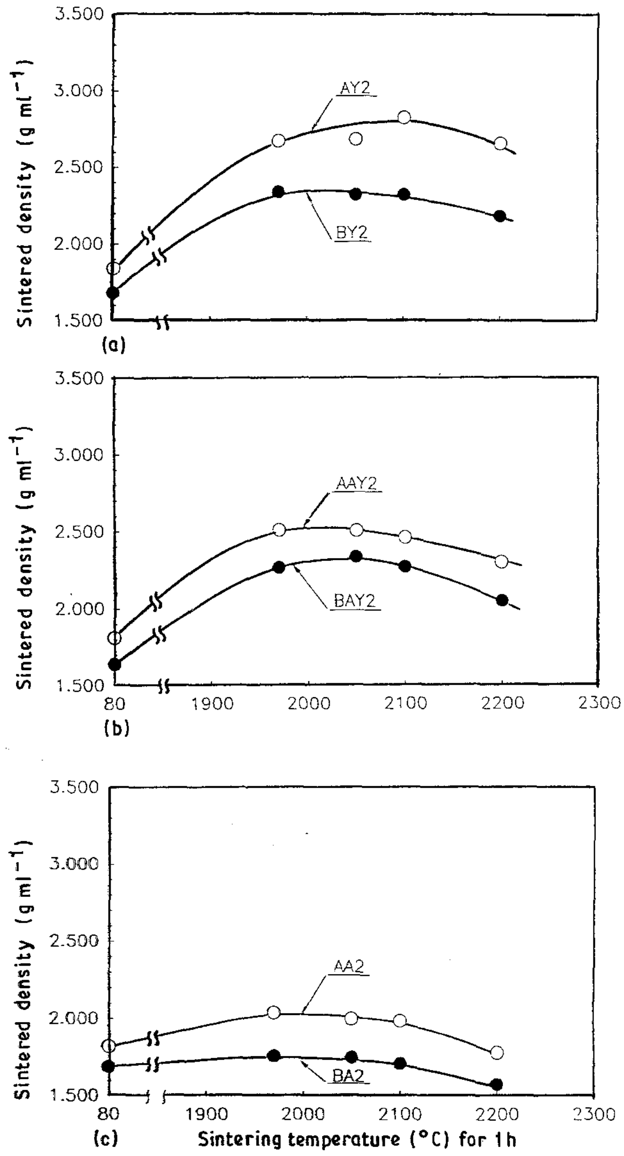

Figure 1 Density of AlN–SiC ceramics after sintering at 1960–2200 °C in Ar atmosphere without burying in packing powder. (a) 2 wt % yttria sintering aid, (b) 1 wt % yttria, and 1 wt % alumina, (c) 2 wt % alumina.

3.1.4. Amount of sintering aids

The sintered density of AlN–SiC composites with more yttria sintering aid (4 wt %) are summarized in Fig. 2. Almost 98.5% TD can be achieved when AY4 is sintered at 2050–2100 °C, higher than the density of

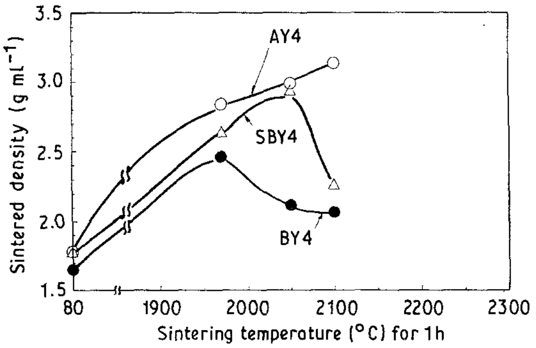

Figure 2 Density of AlN–SiC ceramics with 4 wt % yttria sintering aid at different temperatures without using packing powders.

the composites with 2 wt % yttria (AY2). Therefore, 4 wt% yttria is required for SiC–AlN composites to achieve high density when packing powder is not used. Fig. 2 also shows that the SiC–AlN composites prepared from alpha-SiC (AY4) have a higher density than the composites prepared from beta-SiC powder (SBY4 and BY4), similar to the results shown in Fig. 1. Moreover, Fig. 2 also reveals that the density of SBY4 and BY4 decreases 10% as the sintering temperature goes higher than 2050 °C. The surface of these samples was found to have a porous layer, especially at the corners of the sintered pieces. The decrease in density at higher temperature is due to this porous layer. Microstructure and EDS characterization of these areas are discussed in the following sections.

3.1.5. *Sintering time*

Fig. 3 shows the densities of AlN–SiC ceramics after sintering at 2050 °C for 1, 2 and 4 h. These results indicate that 1–2 h is an optimum sintering period. Longer sintering time does not improve the sintered density.

3.1.6. *Packing powder*

All the data shown in Figs 1–3 are for the density of AlN–SiC composites sintered without using packing powders. Under these firing conditions, a degradation layer was always observed at the surface of the samples. To avoid this degradation layer, two different types of packing powder, beta-pp and alpha-pp, were used. Beta-pp is composed of 50 wt % beta-SiC and 50 wt % AlN, and alpha is composed of 50 wt % alpha-SiC and 50 wt % AlN. The sintered densities of several SiC–AlN composites with or without using packing powder are summarized in the Table IV. Alpha-pp packing powder effectively improved the sintered density of composites. For example, the density of AY2 was increased from 2.99 g cm^{-3} to 3.18 g cm^{-3} when alpha-pp packing powder was used. The degradation layer in the samples fired with alpha-pp packing powder was also found to be greatly reduced. Table IV also shows that beta-pp packing powder did not work as well as alpha-packing powder. Further study is required to understand this difference.

Table IV also shows that yttria (AY2) is a better sintering aid than alumina (AA2) or calcia (AC2). Moreover, under the sintering conditions using packing powder, only 2 wt % yttria is required to yield a high density of AlN–SiC composites (AY2).

3.1.7. *Sintering temperature for the composites with different AlN/SiC ratios*

The results and discussion above cover the composites with a one-to-one AlN/SiC ratio. After identifying the optimum sintering aid, the amount of sintering aid, the sintering time and the sintering condition, composites with different AlN/SiC ratios were prepared. A sintering aid of 2 wt % yttria and alpha-pp packing powder was used during sintering. The sintered densities of composites with different AlN/SiC ratios after firing at a temperature between 1920 and 2100 °C are summarized in Fig. 4. Different composites were found to have different optimum sintering temperatures. The composites rich in AlN (7/3 Y2) can be densified at a temperature as low as 1920 °C; but for the composites rich in SiC, higher temperature (2100 °C) is required for achieving high density. Nevertheless, all the SiC–AlN composites can be sintered to high density at temperatures between 2050 and 2100 °C when 2 wt % yttria and packing powder were used.

3.2. Microstructure and phase characterization

3.2.1. *Optical microscopy*

The optical microstructure of polished and then etched AlN–SiC composites is shown in Fig. 5. This

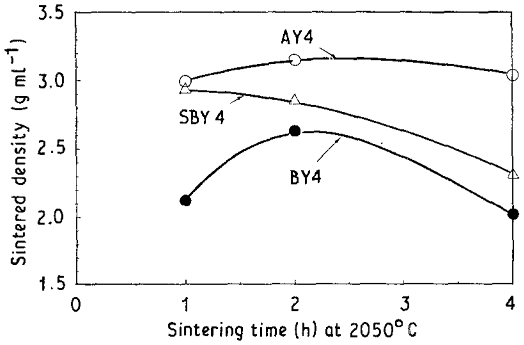

Figure 3 Density of composites with 4 wt % sintering aid at 2050 °C for various times.

TABLE IV Density of AlN–SiC alloys after sintering at 2050 °C for 2 h, with or without packing powders

Sample	Density (g cm^{-3})		
	No Packing	In beta-pp	In alpha-pp
AY4	3.15	3.15	3.20
BY4	2.63	2.76	3.08
SBY4	2.86	2.98	3.18
AY2	2.99	2.82	3.18
BY2	2.49	2.51	2.78
AAY2	2.61	2.60	2.89
BAY2	2.44	2.39	2.63
AA2	1.95	–	2.01
AC2	–	–	2.12

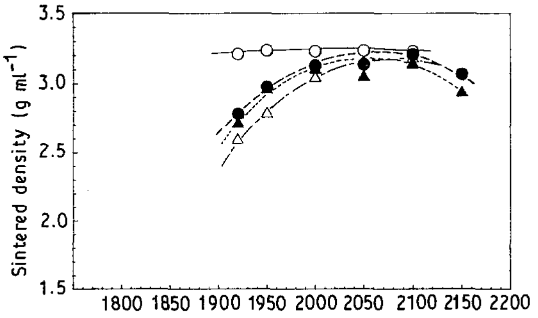

Figure 4 Density of SiC–AlN ceramics after sintering at different temperatures with samples buried in packing powder. (○) 7/3Y2, (●) AY2, (△) 3/7Y2, (▲) SBY2.

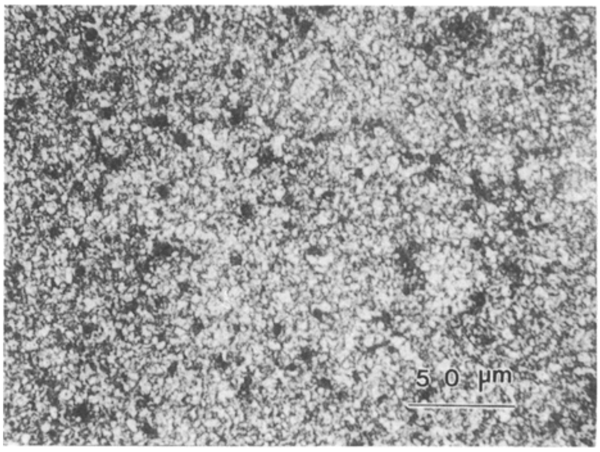

Figure 5 Optical micrograph of SBY4 showing 3–5 µm grain size.

figure reveals highly dense and homogeneous microstructure. The grain size is about 3–5 µm.

3.2.2. SEM and EDS

As discussed in Section 3.1, SiC–AlN composites had a serious degradation layer when they were sintered without using packing powder. SEM and EDS were used to characterize this layer. As shown in Fig. 6, this degradation layer was found to be more porous than the centre of the sample. Moreover, EDS showed this porous layer to be rich in SiC as compared with the composition at the centre of the specimen (see Fig. 7). These results suggest that the decomposition of AlN at high temperature causes the porous degradation layer when the samples are sintered without using packing powder. The packing powder provides a local AlN-rich atmosphere which protects the samples from decomposition and thus increases the sintered density.

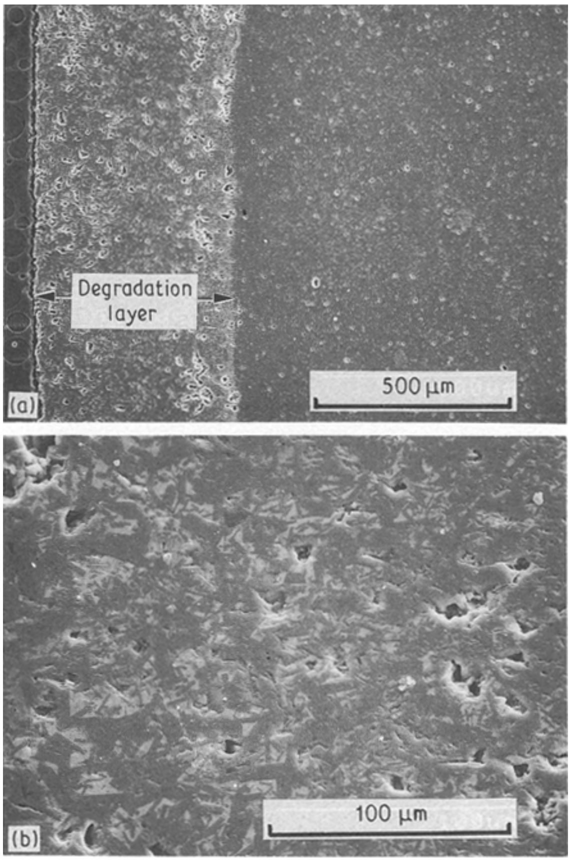

Figure 6 Scanning electron micrograph showing surface degradation of sample AY4 (a) after sintering at 2050 °C for 4 h without using packing powder, (b) higher magnification at the surface layer.

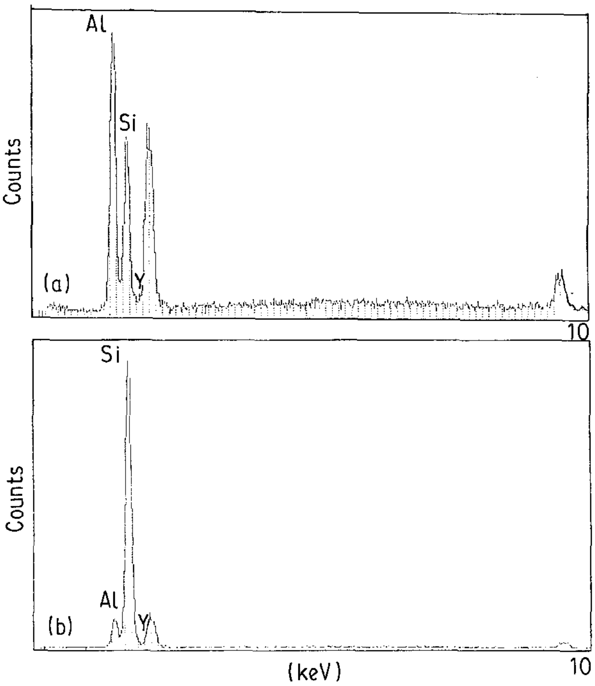

Figure 7 EDS spectra of central and edge area in Fig. 6a, (a) central, and (b) edge area.

3.2.3. XRD analysis

As discussed in the previous section, the optimum sintering temperature of SiC–AlN alloys was about 2050–2100 °C. The specimens sintered in this temperature range without using packing powder had a surface degradation layer, which was rich in yttrium and silicon (see Fig. 7). The X-ray diffractometry analysis on the as-fired surface and ground surface are shown in Table V. The major phase in the as-fired surface was 6H and the minor phases were 2H and 15R. After the degradation layer was polished away, the ground surface showed a major 2H phase and minor 6H and 15R phases. When packing powders

TABLE V Phase of AlN–SiC alloys after sintering at 2050 °C with or without packing powders

Sample	Firing conditions	Phases	
		As-fired surface	Ground surface
AY4	2050 °C, 2 h no packing powder	Major: 6H Minor: 2H, 15R	Major: 2H (split) Minor: 6H, 15R
	2050 °C, 2 h alpha packing powder	Major: 2H (split) Minor: 6H, 15R	Major: 2H (split) Minor: 6H, 15R

were used, the degradation layer could be reduced and the as-fired surface had similar phases at the centre of the specimens. The (0 0 2) peaks in the X-ray diffraction patterns of Fig. 8 also revealed that the as-fired surface of the alloys sintered without using packing powder had stronger SiC peaks than AlN peaks, indicating that AlN might decompose and evaporate from the surface at high temperature and matching the EDS results in the previous section. The packing powder could reduce this decomposition reaction, and therefore the surface would have similar phases as exist inside, and higher overall density.

3.2.4. (TEM)

The X-ray diffraction patterns showed multi-phase after the materials were sintered at 2100 °C. Under the TEM at high magnification, the microstructure was found to be composed of large AlN–SiC solid solution grains, small SiC-rich grains and an yttria-rich grain-boundary phase as shown in Fig. 9. The EDS characterization on the area of Fig. 9a shows that large AlN grains contain a certain amount of SiC, but small SiC grains do not contain much AlN (Fig. 9b and c), indicating that the SiC diffusion rate in the AlN is faster than that of AlN in the SiC grains. These results also imply that SiC-rich SiC–AlN composites will need a higher temperature and a longer time to achieve single solid solution. The detailed microstructure and phase transformation during post-sintering heat treatment to achieve single solid solution and then *in situ* reinforced microstructure will be discussed in a forthcoming paper [22].

Most of the grain-boundary phase was found to be concentrated at the triple junction of grains, especially in the region of an SiC cluster (see Fig. 10). EDS results show that the grain-boundary phase in the pocket contained Y, Si, Al, O and N, suggesting that yttria sintering aid reacts with AlN and SiC during sintering and thus assists in densification through the liquid phase.

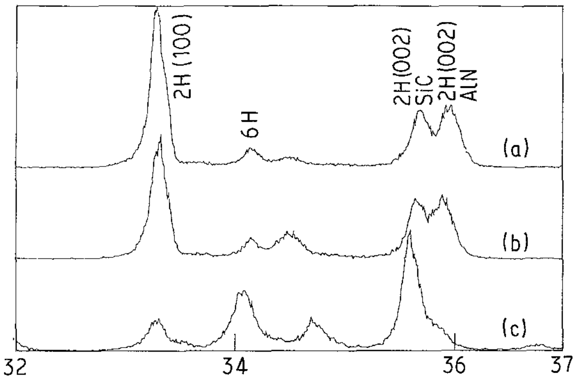

Figure 8 XRD patterns of the as-fired surfaces of AY4, (a) in beta-SiC and AlN packing powders, (b) in alpha-SiC and AlN packing powders, and (c) no packing powder.

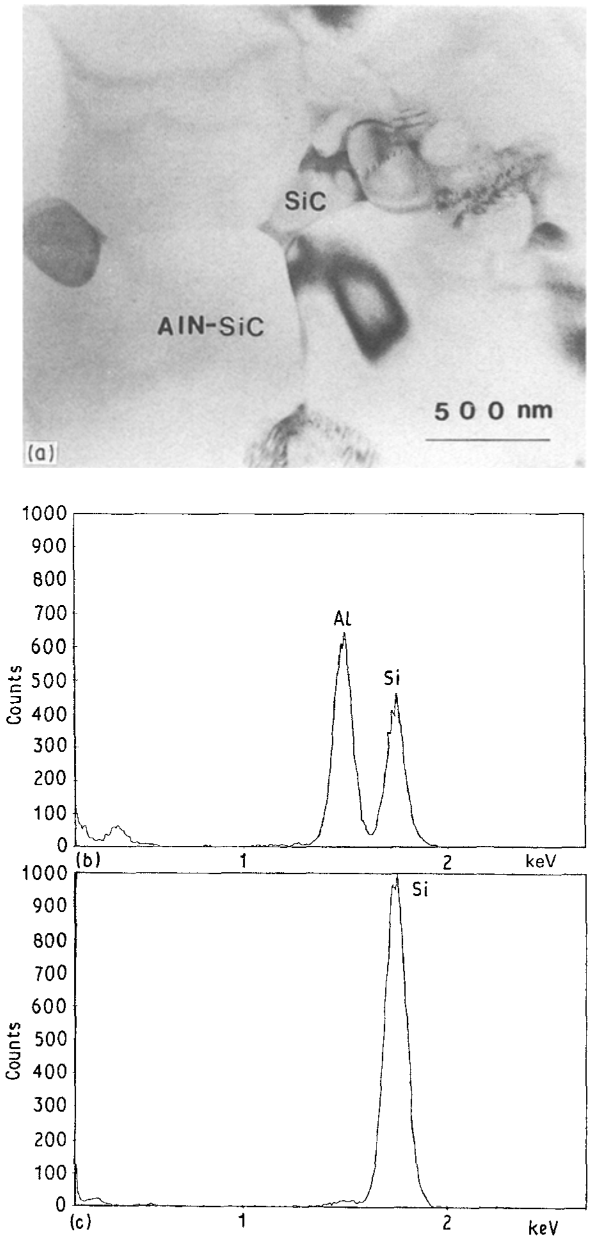

Figure 9 AY4 after sintering at 2100 °C for 1 h. (a) Transmission electron micrograph showing large AlN–SiC grains and small SiC-rich grains, (b) EDS results on the large grains, and (c) EDS on the small grains.

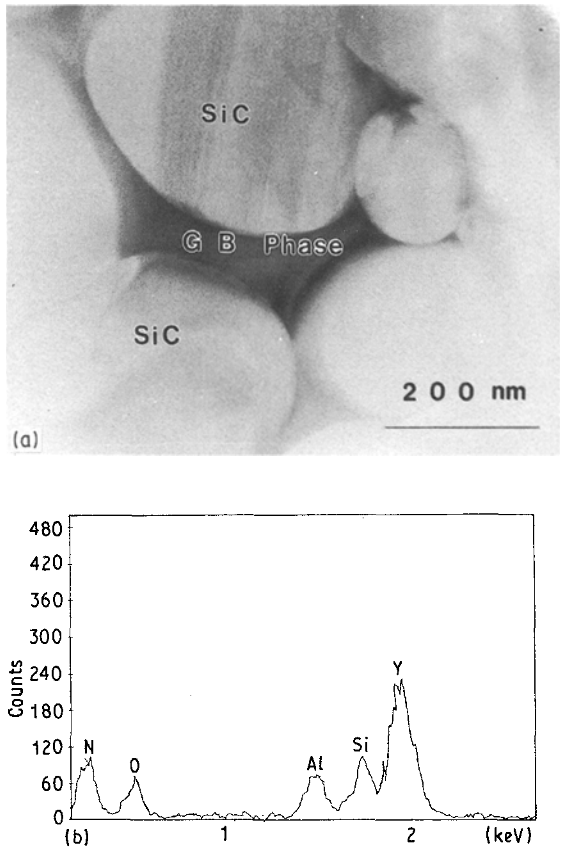

Figure 10 The SiC-rich area and grain-boundary phase. (a) Transmission electron micrograph, (b) EDS result on the grain-boundary phase.

4. Conclusions

The SiC–AlN ceramic composites made from commercial SiC and AlN powders have been successfully pressureless sintered with an optimum amount of sintering aids. Yttria was found to be a better sintering aid than alumina or calcia. Only 2 wt % yttria is required to achieve high density. The yttria sintering aid reacts with AlN and SiC powders and forms a Y–Si–Al–O–N liquid phase to assist densification during pressureless sintering. Both alpha and beta SiC powders can be used to prepare high-density SiC–AlN composites, although alpha-SiC can yield a slightly higher density.

Packing powder plays an important role in achieving high-density SiC–AlN. The composites sintered without using packing powder always have a porous degradation layer. The porous layer is rich in SiC, suggesting that the decomposition of AlN at high temperature is the major cause for this layer. Packing powder can improve the overall density by preventing the formation of this degradation layer through providing a localized AlN-rich atmosphere.

The composites with different AlN/SiC ratio have different optimum sintering temperatures for achieving high density. The composite with higher AlN content can be densified at lower temperatures. However, all of the composites can achieve high density at 2050–2100 °C. At these temperatures, 1–2 h is the optimum sintering period for densification. After sintering, the composites have SiC–AlN solid solution grains and submicrometre SiC-rich grains.

Acknowledgements

This research was partially supported by the Air Force Office of Scientific Research under Contract F49620-88-C-0104. The authors thank Dr James D. Hodge and Dr John W. Halloran, CPS Superconductor Corporation, for their inspiration and helpful discussion. Special thanks are due to the committee of the User Center, HTML, which allowed us to use advanced analytical equipment, and to the following who assisted us in the operation of the instruments, Dr C. Hubbard, Mr B. Cavin and Ms K. More. This research was performed while Wen-Cheng J. Wei was associated with Ceramics Process Systems Corporation.

References

1. I. B. CUTLER, P. D. MILLER, W. RAFANIELLO, H. K. PARK, D. P. THOMPSON and K. H. JACK, *Nature* **275** (1978) 434.
2. W. RAFANIELLO, K. CHO and A. V. VIRKAR, *J. Mater. Sci.* **16** (1981) 3479.
3. R. RUH and A. ZANGVIL, *J. Amer. Ceram. Soc.* **65** (1982) 260.
4. W. RAFANIELLO, M. R. PLICHTA and A. V. VIRKAR, *ibid.* **66** (1983) 272.
5. K. TSUKUMA, M. SHIMADA and M. KOIZUMI, *J. Mater. Sci. Lett.* **1** (1982) 9.
6. M. SHIMADA, K. SASAKI and M. KOIZUMI, in "Processing of International Symposium on Ceramic components for Engine", edited by S. Somiya, E. Kanai and K. Ando (KTK Scientific Publishers, Tokyo, Japan, 1983) pp. 466–72.
7. A. ZANGVIL and R. RUH, *J. Mater. Sci. Lett.* **3** (1985) 249.
8. *Idem.*, *Mater. Sci. Engng* **71** (1985) 159.
9. R. RUH, A. ZANGVIL and J. BARLOWE, *Amer. Ceram. Soc. Bull.* **64** (1985) 1368.
10. S. Y. KUO, Z. C. JOU, A. V. VIRKAR and W. RAFANIELLO, *J. Mater. Sci.* **21** (1986) 3019.
11. Z. C. JOU, S. Y. KUO and A. V. VIRKAR, *ibid.* **21** (1986) 3015.
12. *Idem.*, *J. Amer. Ceram. Soc.* **69** (1986) C-279.
13. J.-L. HUANG, A. C. HURFORD, R. A. CUTLER and A. V. VIRKAR, *J. Mater. Sci.* **21** (1986) 1448.
14. S. Y. KUO and A. V. VIRKAR, *J. Amer. Ceram. Soc.* **70** (1987) C-125.
15. W. T. DONLON, J. HANGAS, C. R. PETERS, S. SHINOZAKI and K. MAEDA, For abstract see no. 21-BP-88, presented at the American Ceramic Society Annual Meeting (1988).
16. A. ZANGVIL and R. RUH, *J. Amer. Ceram. Soc.* **71** (1988) 884.
17. W. BOCKER and H. HAUSNER, *Powder Metall. Int.* **11** (1979).
18. K. KOMEYA, *Amer. Ceram. Soc. Bull.* **63** (1984) 1158.
19. S. PROCHAZKA, *Special Ceram.* **6** (June) (1975) 171–82.
20. A. H. HEUER, G. A. FRYBURG, L. U. OGBUJI, T. E. MITCHELL and S. SHINOZAKI, *J. Amer. Ceram. Soc.* **61** (1978) 406–412.
21. T. E. MITCHEL, L. U. OGBUJI and A. H. HEUER, *ibid. J. Amer. Ceram. Soc.* **61** (1978) 412–413.
22. R.-R. LEE and W.-C. J. WEI, *Ceram. Eng. Sci. Proc.* **11 (7–8)** (1990) 1094–1121.

Received 14 February
and accepted 4 September 1990